Science of the Total Environment 884 (2023) 163720

Contents lists available at ScienceDirect

Science of the Total Environment

journal homepage: www.elsevier.com/locate/scitotenv

Scavenging of polystyrene microplastics by sediment particles in both turbulent and calm aquatic environments

T. Serra *, J. Colomer

Department of Physics, Escola Politècnica Superior, University of Girona, Campus Montilivi, 17003 Girona, Spain

HIGHLIGHTS

- Fast-settling sediment particles scavenge slow-settling MP particles.
- The scavenging of MP by sediment increases the MP pollution in sediment beds.
- In calm zones the scavenging of MP by sediments is greater than in mixing zones.
- Water salinity does not effect the scavenging of MP by sediment particles.

GRAPHICAL ABSTRACT

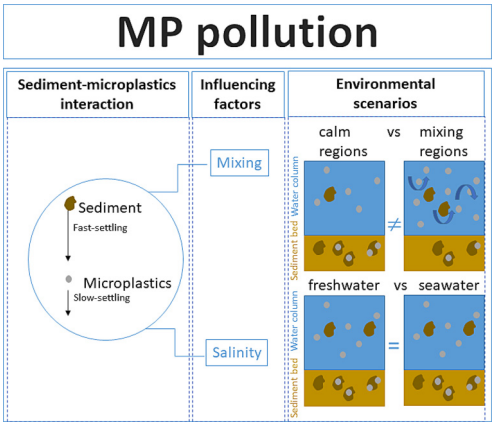

ARTICLE INFO

Editor: Damia Barcelo

Keywords:
Deposition
Transport
Shear rate
Oscillating grid
Salinity

ABSTRACT

Microplastic particles (MP) are emerging pollutants ubiquitously distributed in all aquatic environments, remaining in suspension in the water column or deposited in sediment beds. MP are suspended in the water column along with other particles with whom they might interact. The current study presents the results of slow-settling MP (Polystyrene) scavenged by fast-settling sediment particles. The study covers a wide range of salinities (from freshwater to saltwater) and shear rates (from calm to mixing ecosystems). In calm regions, the scavenging by fast-settling sediment particles produces the greatest removal of MP from the water column (42 % of MP in suspension), thus increasing the MP pollution of sediment beds. In contrast, turbulence reduces the settling of MP and sediment particles (72 % of MP remain in suspension), causing more pollution than in calm regions.

Although salinity increased the buoyancy of MP, the scavenging by sediment has been found to overcome the increase in buoyancy. Consequently, MP are transported to the sediment bed independently on the salinity. Therefore hotspots of MP contamination in aquatic environments need to consider both the MP and sediment interaction and the local mixing of the water column.

1. Introduction

In recent decades plastic production has increased exponentially (Ostle et al., 2019), with plastic packaging, personal care, cosmetic, and industrial products dominating the plastics in use in our daily lives. MP subsequently end up as emerging pollutants in rivers, wastewater treatment plants and

* Corresponding author.
E-mail address: teresa.serra@udg.edu (T. Serra).

http://dx.doi.org/10.1016/j.scitotenv.2023.163720
Received 6 February 2023; Received in revised form 3 April 2023; Accepted 21 April 2023
Available online 1 May 2023

eventually in marine aquatic systems (Li et al., 2019a; Li et al., 2019b; Mao et al., 2020; Ostle et al., 2019; Sun et al., 2019), where they may cause physical and chemical risk to organisms (Magester et al., 2022; Tosetto et al., 2016). The quantity of plastic debris is greater near urban centres and frequented beaches (Thompson et al., 2009), posing a serious problem for freshwater, coastal and ocean environments.

Due to their density, most of the plastics remain in the top layers of the ocean where wind and waves, together with sunlight radiation, deteriorate, break down and erode them into microscopic plastic particles (known as MP) below 5 mm in size (Li et al., 2019a; Li et al., 2019b). MP particles have also been found in the sediment of coastal zones ((Andradi, 2011); Thompson, 2004) and also in deep ocean sediment (Van Cauwenberghe et al., 2013) as well as shore and lake bottom sediment (Hengstmann et al., 2021; Mao et al., 2020) and river sediments (Xia et al., 2021). In both lake and sea waters, MP may form aggregates with other particles (heteroaggregation) due to continuous mixing (Li et al., 2019a; Li et al., 2019b), resulting in a complex particle heterointeraction, also impacting on the vertical transport of MP and their long-term distribution. The presence of salts and surfactants can alter the surface properties of MP, neutralising the electric double layer and leading to further aggregation and the formation of larger aggregates (Li et al., 2019a; Li et al., 2019b; Serra et al., 1997). Heteroaggregates of MP will be ingested by phytoplankton grazers and higher trophic levels, due to their small dimensions (Long et al., 2015; Van Cauwenberghe et al., 2013). MP can absorb heavy metals and organic pollutants from the environment, as well as toxic chemicals used as additives in the production process (Mao et al., 2020). Biofouling can also impact on the transport of MP in the water column. For example, phytoplankton cells attached to buoyant MP particles have been found to increase the density of plastic debris (Long et al., 2015), thus increasing the transport of MP to the bottom of the water column. For instance, the aggregation of polyethylene particles together with organic matter, cyanobacteria, and iron minerals, resulted in an increase in the sinking rates of MP in a stratified reservoir (Leiser et al., 2020).

The presence of sediment particles in the water column might also enhance the transport of MP in the water column, through aggregation or scavenging of small MP particles by sediments. In such cases, buoyant and settling MP particles are prone to being transported to the bottom of a water column due to the heteroaggregation. Recently, Leiser et al. (Leiser et al., 2020) found buoyant polyethylene MP were incorporated into sinking-organic aggregates, followed by deposition into sediment freshwater ecosystems. The accumulation of MP in lakebed and seabed sediments has been largely reported to affect benthic organisms (Bellasi et al., 2020; Ivar do Sul and Costa, 2014). Although no effect of MP has been found in the survival of most benthic organisms (such as, for example, *Gammarus pulex*), MP have been found to impact their behavior (Redondo-Hasslerham et al., 2018). The most spread synthetic plastics are low- and high-density polyethylene (PE), polypropylene (PP), polyvinyl chloride (PVC), polystyrene (PS) and polyethylene terephthalate (PET). PS is the third MP in terms of global waste generation after PP and PE, with 17 million tonnes per year (Yuan et al., 2022). Facial and hand cleansers containing PS microplarticles are widely used, especially in developed countries. Since PS are not retained in wastewater treatment plants they represent a postconsumer product entering in river and marine ecosystems (Gregory, 1996; (Ivar do Sul and Costa, 2014)).

Considering all the above-mentioned evidence that MP accumulate in the sediment beds of water bodies, the mechanisms that determine the vertical transport of MP in the water column need to be better studied. In particular, the role sediment particles play in the scavenging of MP in calm or mixing environments and salty or freshwater environments is still poorly understood. The persistence and transport of MP through the water column is crucial to determine their fate and their possible impact on natural environments. Microplastic particles are known to accumulate in bottom sediments of continental shelfs (Thompson et al., 2004) and also deep sediment beds in the open ocean (Van Cauwenberghe et al., 2013). Turbidity currents are known to be important agents in transporting microplastic particles to the seabed (Pohl et al., 2020) and some models predict also accumulation of MP in regions, where there is a higher concentration of suspended fine sediment particles (Shiravani et al., 2023). Although the scavenging of MP particles by sediments has been studied previously in the laboratory under calm conditions (Li et al., 2019a; Li et al., 2019b), the effect of turbulence and salinity remains unknown. In some situations, some of the most abundant and recalcitrant MP persist in suspension in the water column against what was expected (Erni-Cassola et al., 2019). High concentrations of salt enhance the buoyancy of particles and increase the amount of particles in suspension. Furthermore, high turbulence levels are expected to produce more resuspension and also increase the number of particles in suspension compared to calm zones. Therefore, the mechanisms that contribute to transporting MP in the water column are needed to be understood to determine the balance of MP in aquatic systems. The aim of this study is to find the role sediment play in the transport of MP (specifically PS microspheres) along the water column under different environmental salinity and mixing conditions. To fulfil this objective, the following hypothesis were tested: (1) salinity promotes heteroaggregation between sediment and MP particles; (2) in environments with MP only, mixing reduces the settling rates of MP, and (3) in mixing environments, sedimentation of heteroaggregates dominates over resuspension, leading to greater removals of MP due to scavenging by sediment particles.

2. Methodology

2.1. Calculation of the oscillating grid shear rate

An oscillating grid device (OGT) was used to generate a range of turbulent shear rates (i.e. mixing levels). Oscillating grid devices have largely been used to mimic turbulence in natural environments since they provide a power decay of the turbulent kinetic energy with distance from the forcing agent, in this case the grid (Serra et al., 2008). For example, Pujol et al. (Pujol et al., 2012) used an oscillating grid to study the attenuation of turbulence inside a submerged aquatic canopy, Serra et al. (Serra et al., 2008) used an oscillating grid to study the aggregation of microplastic particles and Colomer et al. (Colomer et al., 2019) used an oscillating grid to determine the resuspension of sediment from a sediment bed. An OGT consists of a horizontal grid shaft connected to a motor through a vertical axis (Fig. 1). To have three replicates of the experiments, in the current study the motor was connected to a frame holding three grid shafts. As a result, three replicate recipients could be conducted simultaneously (Serra

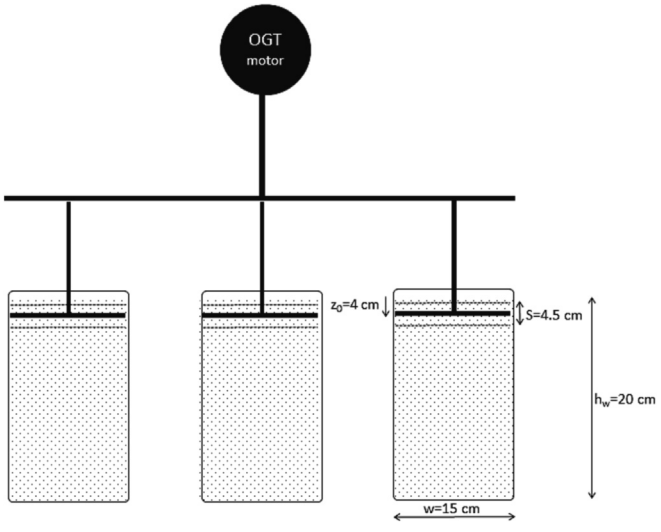

Fig. 1. Scheme of the experimental set up: h_w is the water height, S is the stroke of the oscillating grid device, and z_0 is the initial position of the grid in the vertical axis (z). The three reactors were used simultaneously to have three different replicas of each experimental condition.

et al., 2019) for each experimental condition. Each recipient had a capacity of 3.5 L, a radius of 15 cm and a height of 17 cm. To fit into each reactor, grids were circular shaped, 14 cm in diameter and made of cylindrical stainless steel bars (Serra et al., 2019). To avoid secondary circulation in the recipient, the gap between the ends of the grid bars and the walls was reduced to 5 mm, i.e., the minimum possible (Serra et al., 2008).The grid had a mesh spacing of M = 1 cm.

In Fig. 1 a schematic view of the oscillating grid system is shown, where the depth of the working fluid (h_w = 20 cm), the distance between the top of the recipient and the highest position of the grid (z_0 = 4 cm), the recipient diameter (w = 15 cm) and the distance coursed by the grid (S = 4.5 cm) are shown.

The controlling motor was connected to a variable power supply that was switched to different voltages, resulting in different oscillating frequencies (f, in s^{-1}). The mean shear rate along the total working depth ($\overline{G}$, in s^{-1}) was calculated using the grid characteristics, the oscillating frequency of the grid, and the height of the working fluid h_w (Serra et al., 2008) as follows:

$$\overline{G} = \frac{1}{h - z_0}\int_{z_0}^{h_w} 0.0458 f^{\frac{3}{2}} z^{-2} = 0.0458 f^{\frac{3}{2}} (h_w z_0)^{-1} \quad (1)$$

Hereafter, the mean shear rate $\overline{G}$ will be known as G. For the frequency studied and the grid characteristics, G was found to be in the range of 0 to 40 s^{-1} (Table 1, supplementary material). In accordance with the equation used by Geyer et al. (Geyer et al., 2008), the dissipation rate (ε, in W Kg^{-1}) can be calculated (see Table 1, supplementary material) according to:

$$\varepsilon = \frac{G^2 \mu}{\rho} \quad (2)$$

where μ was the viscosity (in Pa s) of the water and ρ the density (in kg m^{-3}). From the range of G, the dissipation rate ranged from 0 to 1.55 10^{-3} W/kg (Table 1). Arnott et al. (Arnott et al., 2021) and Peters and Redondo (Peters and Redondo, 1997) found that the dissipation rates (ε) in the ocean are in a range from 10^{-3} to 10^{-5} W/kg, which is consistent with the mixing levels considered in the experiments conducted.

2.2. Measurements of particle concentration

The volumetric particle size distribution of the testing samples was measured by a laser particle size analyser (LISST-100×, Sequoia Inc., US, see the Supplementary Material for more details on the instrument). Both the particle volume concentration and the particle number concentration can be obtained by integrating over a given range of diameters. In the current study, the range between 6 μm and 30 μm will be considered.

2.3. Preparation of the samples

All the experiments were carried out with distilled water. Experiments were performed in 4 L glass beakers filled to 3.5 L (i.e., working volume). To study the dynamics of particles in both freshwaters and seawaters, six salinities were considered for the whole set of experiments (0 ‰, 5 ‰, 10 ‰, 20 ‰, 30 ‰, and 40 ‰). The range of salinities were obtained by simply adding NaCl (PanReac AppliChem, Germany) with the concentration required to the beaker of distilled water and mixed with a mechanical stirrer for 5 min. To ensure a complete homogeneous dilution of the NaCl, the mixture of salt with water was prepared 24 h before starting the experiments.

2.4. Sediment and MP characteristics

The sediment used in this study is a synthetic sediment with ISO 12103-1, A4 Coarse Test Dust specifications. It is made of 69–77 % of quartz (Gmbh and Kg, Germany), 8–14 % of aluminium oxide, 2.5–5.5 % of calcium oxide, 2–5 % of potassium oxide, 1–4 % of sodium oxide, 4–7 % of iron (III) oxide, 1–2 % of magnesium oxide and 0–1 % of titanium dioxide. The density of sediment, as indicated by the technical specifications, ranged between 2500 kg m^{-3} to 2700 kg m^{-3}. Measurements of the Zeta potential for sediment particles (of −8.7 mV, Malvern Zetasizer, Malvern Panalytical, UK) indicated that they are slightly unstable and might present aggregation at an initial stage (Chorom and Rengasamy, 1995). In all the experiments with sediment, 350 mg of sediment were added to the volume of water with salinity and immediately shaken in a bottle to achieve a good mixing of the particles, obtaining a sediment concentration of 25.03 ± 2.45 μL L^{-1} (Fig. 2a). Shortly after shaking the mixture, it was then introduced into each of the three beakers up to the working volume and the first water samples of 100 mL from each beaker were taken and measured with the LISST-100× to obtain the initial particle volume distribution. The MP used in this study are non-functionalized colloidal microspheres

Table 1
Experiments carried out in the laboratory for sediment only (Exp1 to Exp24), MP only (Exp25 to Exp38) and MP and sediment (Exp39 to Exp53). The shear rate (G, in s^{-1}), the salinity (S, in ‰), and the dissipation rate (ε, in Wkg^{-1}) are also presented in the table.

N° of the experiment	Type of particles	G (s^{-1})	S (‰)	$\varepsilon \times 10^{-5}$ (Wkg^{-1})
Exp1	Sediment	0.0	0	0
Exp2	Sediment	0.0	5	0
Exp3	Sediment	0.0	10	0
Exp4	Sediment	0.0	20	0
Exp5	Sediment	0.0	30	0
Exp6	Sediment	0.0	40	0
Exp7	Sediment	5.0	5	2.45
Exp8	Sediment	5.0	20	2.45
Exp9	Sediment	5.0	30	2.45
Exp10	Sediment	5.0	40	2.45
Exp11	Sediment	10.0	30	9.71
Exp12	Sediment	13.0	30	16.4
Exp13	Sediment	20.0	0	39.8
Exp14	Sediment	20.0	5	39.8
Exp15	Sediment	20.0	20	39.8
Exp16	Sediment	20.0	30	39.8
Exp17	Sediment	20.0	40	39.8
Exp18	Sediment	30.0	5	89.5
Exp19	Sediment	30.0	20	89.5
Exp20	Sediment	30.0	30	89.5
Exp21	Sediment	30.0	40	89.5
Exp22	Sediment	40.0	20	155.0
Exp23	Sediment	40.0	30	155.0
Exp24	Sediment	40.0	40	155.0
Exp25	MP	0.0	0	0
Exp26	MP	0.0	5	0
Exp27	MP	0.0	20	0
Exp28	MP	5.0	30	2.45
Exp29	MP	5.0	40	2.45
Exp30	MP	10.0	30	9.71
Exp31	MP	10.0	40	9.71
Exp32	MP	13.0	30	16.4
Exp33	MP	20.0	30	39.8
Exp34	MP	20.0	40	39.8
Exp35	MP	30.0	30	89.5
Exp36	MP	30.0	30	89.5
Exp37	MP	40.0	30	155.0
Exp38	MP	40.0	40	155.0
Exp39	MP + sediment	0.0	10	0
Exp40	MP + sediment	0.0	20	0
Exp41	MP + sediment	0.0	30	0
Exp42	MP + sediment	0.0	40	0
Exp43	MP + sediment	5.0	30	2.45
Exp44	MP + sediment	5.0	40	2.45
Exp45	MP + sediment	10.0	30	9.71
Exp46	MP + sediment	10.0	40	9.71
Exp47	MP + sediment	13.0	30	16.4
Exp48	MP + sediment	20.0	30	38.8
Exp49	MP + sediment	20.0	40	38.8
Exp50	MP + sediment	30.0	30	89.5
Exp51	MP + sediment	30.0	40	89.5
Exp52	MP + sediment	40.0	30	155.0
Exp53	MP + sediment	40.0	40	155.0

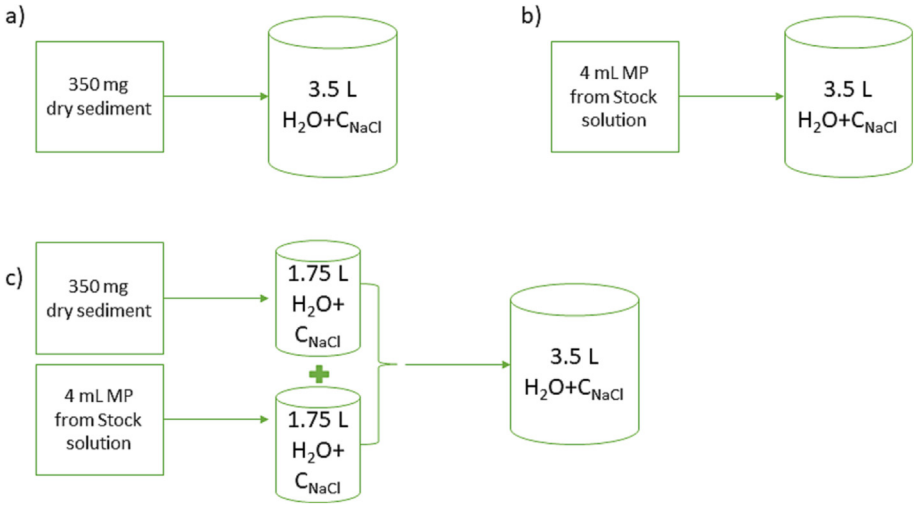

Fig. 2. Scheme of the preparation of the concentrations for the different experiments conducted. a) sediment particles only, b) MP only, c) MP plus sediment.

of polystyrene obtained from the ALPHA Nanotech company (Canada). Following the indications by the manufacturer, the Zeta potential of these particles is −18.2 mV, indicating that they are more stable than sediment particles. These particles do not destabilize in a saltwater suspension and therefore they do not aggregate with themselves. Since they are Polystyrene particles, their density is 1050 kg m^{-3}. In all the experiments with MP, a volume of 4 mL of MP was taken from the stock bottle and introduced into the beaker with the previously prepared saltwater, and stirred together to obtain a homogeneous distribution of the MP particles obtaining a concentration of 13.93 ± 2.40 μL L^{-1} (Fig. 2b). As in the previous experiments with sediment, a 100 mL sample from each beaker was collected and the initial particle volume distribution was measured and then returned to the beaker.

2.5. MP and sediment experiments

A total of 53 experiments were carried out in the study (Table 1, supplementary material). These experiments encompassed six salinities (from 0 to 40 ppm) and seven shear rates (between 0 and 40 s^{-1}) for each type of particle: sediment-only, microplastics (MP), and sediment plus microplastics (MP + sediment). For all the experiments with MP and sediment, four mL of MP from the stock solution were introduced and mixed into half of the total working volume (of 1.75 L) and then 350 mg of sediment were introduced and mixed in the other half of the working volume (of 1.75 L), see Fig. 2c. After reaching a homogeneous mixture, both volumes were merged and mixed again. The initial particle volume distribution was also measured and returned to the beaker as had been previously done for the other with sediment-only and MP-only experiments. Shortly after the measurement, the grid was situated in the beaker, the frequency adjusted accordingly, and the experiment initiated.

2.6. Particle size distribution of sediment and MP

Measurements of the particle size distribution indicated that sediment ranged from 10 μm to 100 μm (Fig. 3a) and that polystyrene MP particles range from 6 μm to 30 μm, with a maximum in the particle size distribution centred at 10 μm (Fig. 3a). The cumulative particle size distribution of sediment and MP indicated that MP had a median of 11.15 μm (Fig. 3b) while sediment presented a larger median of 53.5 μm (Fig. 3b), also in accordance with the technical characteristics of these particles. The median of the sediment used in the current study is close to that observed in suspended sediment in coastal river plumes (Pitarch et al., 2019). In their case, d_{50} varied in the range 65 μm to 40 μm, decreasing with distance from the coast. The MP particles are spherical that can be ubiquitously in many aquatic ecosystems and in the range of sizes ingested by aquatic organisms (Cole et al., 2013). In addition, polystyrene is the fourth most commonly produced polymer and its presence in aquatic ecosystems has been frequently reported (Hidalgo-Ruz et al., 2012; Browne et al., 2010).

2.7. Measuring technique

The grid was situated at its position at the top of the beaker and the oscillating movement was initiated at the frequency required for each experiment. To observe the structural characteristics of the settled particles, three microscope glass cover plates were fixed on the bottom of the beaker with double-sized tape. Their small thickness ensured a reduced interference in the hydrodynamics of the flow. These glass cover plates were removed at the end of each experiment and observed using a scan electron microscope at the University of Girona (UdG) facilities.

Each experiment was run for 120 min. During the first hour of the experiment, a sample of 100 mL of each replicate was pipetted every 15 min and measured with the LISST-100× to obtain the temporal evolution of the particle size distribution and concentration. The pipette used was cut midway in order to reduce the effect of the water sampling (Serra et al., 2008). The sample was measured and then carefully introduced back into the beaker without switching off the OGT in order to maintain the same working volume throughout the experiment. After the first hour, measurements were taken every 30 min until the 120 min that experiments lasted. In all the cases except for those corresponding to G = 0 s^{-1} (Fig. 1 of the supplementary material), the steady state was reached after 90 min of running the experiment. However, for the purpose of comparison between experiments the same t = 90 min was considered also for G = 0 s^{-1}.

To determine the volumetric concentration of MP particles at a certain time (c), the concentration measured by the LISST-100× for all the particles in the range of 6 μm to 30 μm was calculated. For the sediment particles, the concentration of sediment for the same range was considered as a proxy to determine the temporal evolution of sediment particles in the system. Likewise, the MP + sediment concentration was also calculated for the same range. Since MP have a much higher concentration of particles in this particle range than sediment, it is expected to represent the behavior of MP. The ratio between c (the concentration at time t) and c_0 (the initial particle volume concentration) was calculated.

2.8. Theory

The rate of particle decrease in the water column (c/c_0) is expected to follow an exponential decay with time (t) according to the equation:

$$\frac{c}{c_0} = e^{k_t t} \tag{3}$$

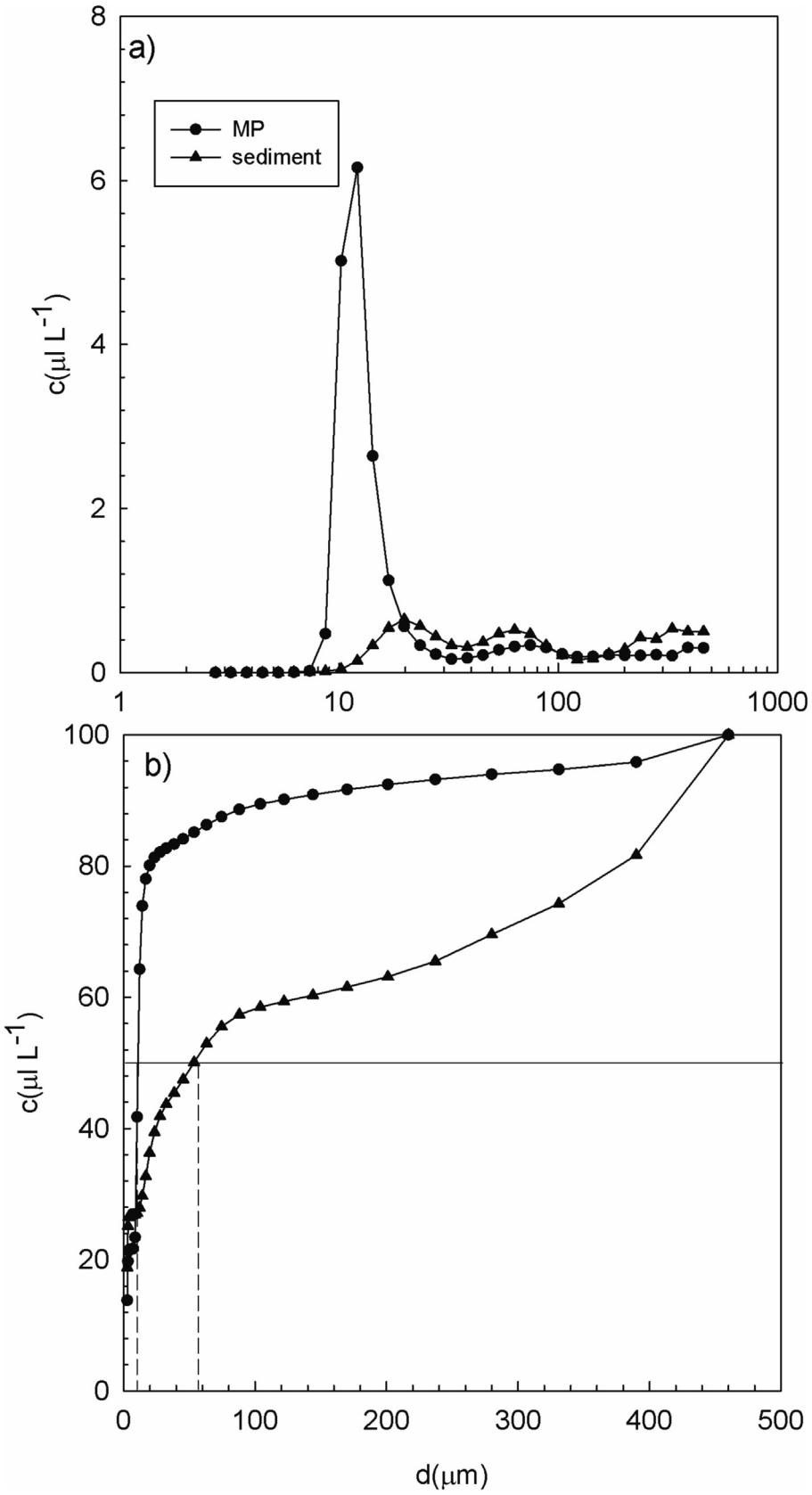

Fig. 3. a) Particle volume concentration versus the particle diameter for both MP and sediment particles measured at $t = 0$ s. b) Cumulative particle size distribution for both MP and sediment particles obtained from data in the Fig. (3a). The horizontal line represents the threshold of 50 % of the cumulative particle size distribution. Vertical dashed lines represent the median of the diameter for MP ($d_{50} = 11.15$ μm) and sediment particles ($d_{50} = 53.5$ μm).

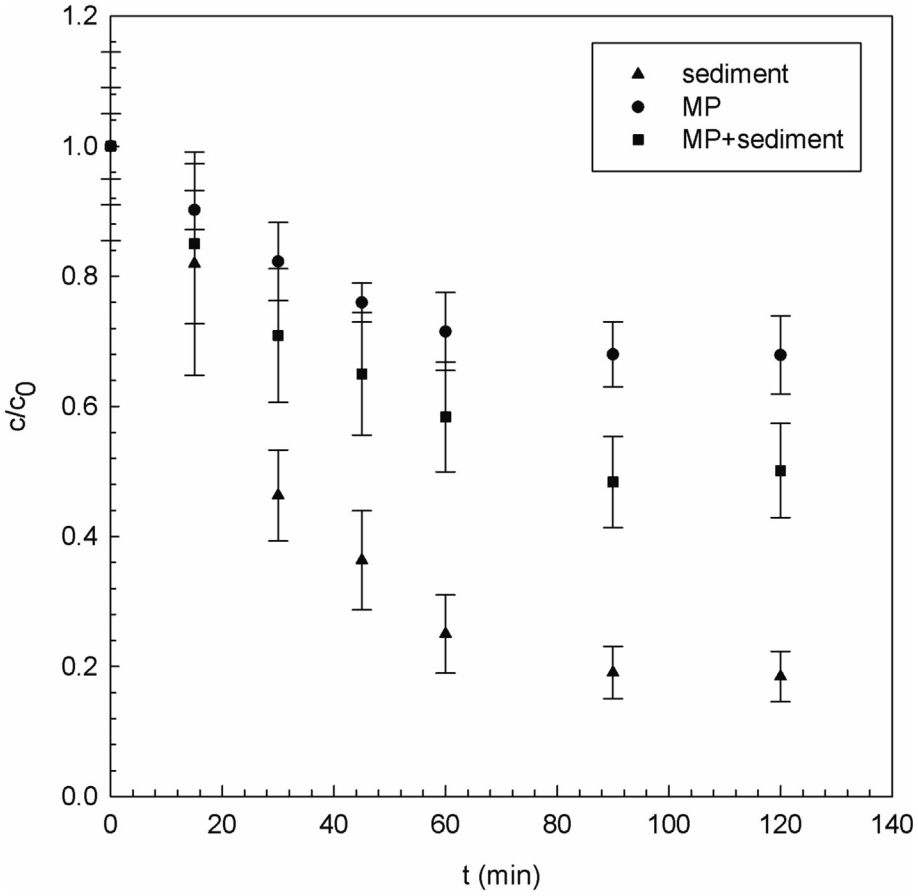

Fig. 4. Temporal evolution of c/c_0 versus t (in min) for the different suspensions of only sediment, only MP, and MP + sediment particles. These results correspond to the experiments carried out at $G = 20\ s^{-1}$ and S = 30 ‰. Vertical error bars represent the standard deviation of the measurements among the three replicas performed.

Where k_t is the total rate of decay (in s^{-1}). In the cases where there was no turbulence (i.e., experiments without shear, i.e., $G = 0\ s^{-1}$), the total rate of decay will be $k_t = -k_s$, where k_s is the sedimentation rate of decay. In experiments with turbulence (i.e., with $G \neq 0\ s^{-1}$), the total rate of decay $k_t = k_{res}\text{-}k_s$, where k_{res} is the resuspension rate of decay. All the rates of decay have units of s^{-1}.

2.9. Quality control and quality assurance

Three replicates of each experimental case were carried out to check for the replicability. The results presented are the average among the three replicates and the standard deviation will be considered the error carried out in the measurement.

Experiments without salt or without shear represent the control experiments that will allow comparison with other experiments conducted with salinity and shear rate.

3. Results

The ratio c/c_0 decreased gradually with time for all three types of particles, presenting an exponential decrease that reached a plateau in all the cases studied (Fig. 4). The temporal decrease of c/c_0 for sediment was faster than that for MP. For the case of MP + sediment, the temporal decrease was lower than for sediment particles, but higher than for MP particles (Fig. 4).

The ratio of the sediment concentration at the steady state $(c/c_0)_{ss}$ increased with the shear rate for all the particles studied (Fig. 5). The highest values of $(c/c_0)_{ss}$ were for the MP-only experiments for all the shear rates tested. In contrast, the lowest values of $(c/c_0)_{ss}$ corresponded to those carried out with sediment only. For experiments conducted with a mixture of MP and sediment, $(c/c_0)_{ss}$ was below that of MP and above that of sediment for all the range of shear rates tested.

The ratio of the sediment concentration at the steady state $(c/c_0)_{ss}$ increased with the salinity for the case of MP. However, for the case of sediment and MP + sediment, $(c/c_0)_{ss}$ remained nearly constant with the salinity (Fig. 6). The ratio $(c/c_0)_{ss}$ for MP presented the highest values compared to the sediment and MP + sediment experiments. MP + sediment presented ratios $(c/c_0)_{ss}$ below those found for MP and above those found for sediment.

The percentage of difference between the concentration of MP in experiments with MP only and those with the combination of MP and sediment particles (MP + sediment) has been calculated and called MP-removal (in percentage):

$$MP - removal(\%) = \frac{(c_{MP} - c_{MP+SED})}{c_{MP}} x100 \quad (4)$$

MP-removal decreased from 40 % to 20 % as G increased from $G = 0\ s^{-1}$ (non-sheared) to $40\ s^{-1}$ (Fig. 7a). No difference was found between the experiments with the different salinities of 30 ‰ and 40 ‰. The removal percentage decreased with G following a power trend, reaching a plateau at $G = 30\ s^{-1}$ with a removal of 20 %, indicating that for $G > 30\ s^{-1}$ the MP-removal percentage remained nearly constant. Photographs of the settled particles at the bottom of the reactors reveal the presence of heteroaggregates between sediment and MP particles at the bottom of the beaker (Fig. 7b).

Following the theory mentioned in the Methodology (Section 2.7) for the cases with $G = 0\ s^{-1}$, the sedimentation rate of decay, k_s has been determined by fitting the experimental data to the model and considering $k_{res} = 0$. For all the salinities studied, k_s for MP (Fig. 8a) is three times

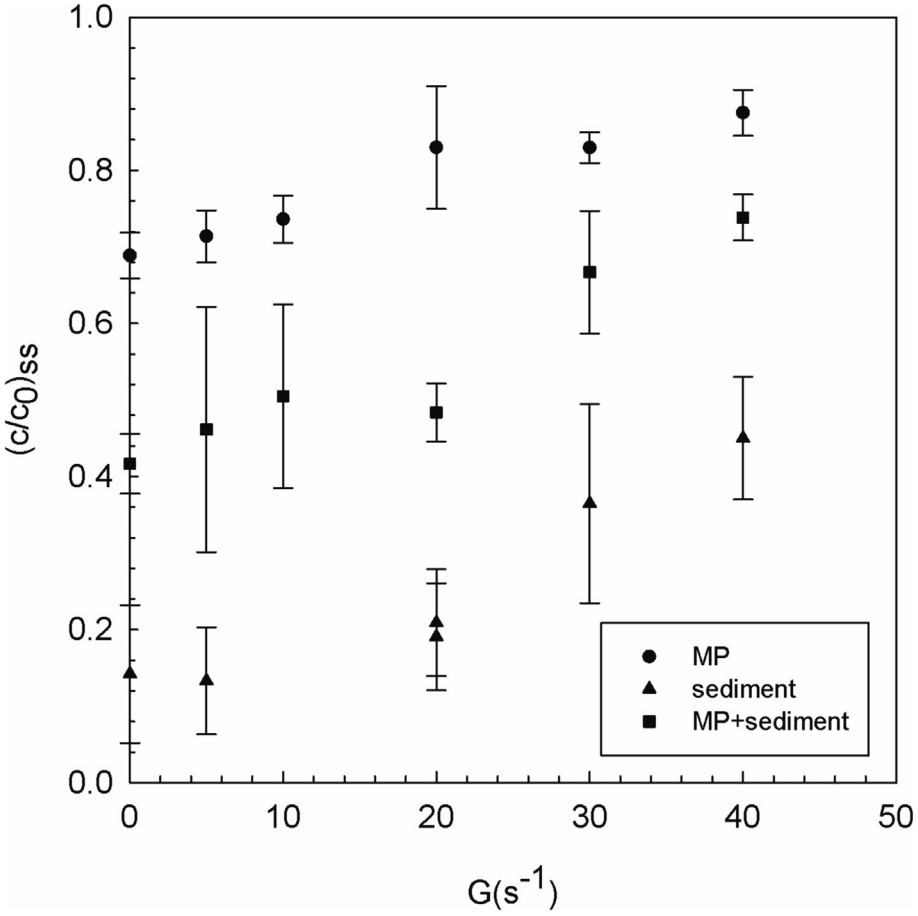

Fig. 5. c/c_0 in the steady state, $(c/c_0)_{ss}$ versus G for S = 40 ‰ for the different types of suspended particles (MP, sediment, and MP + sediment). Vertical error bars represent the standard deviation of the measurements among the three replicas performed.

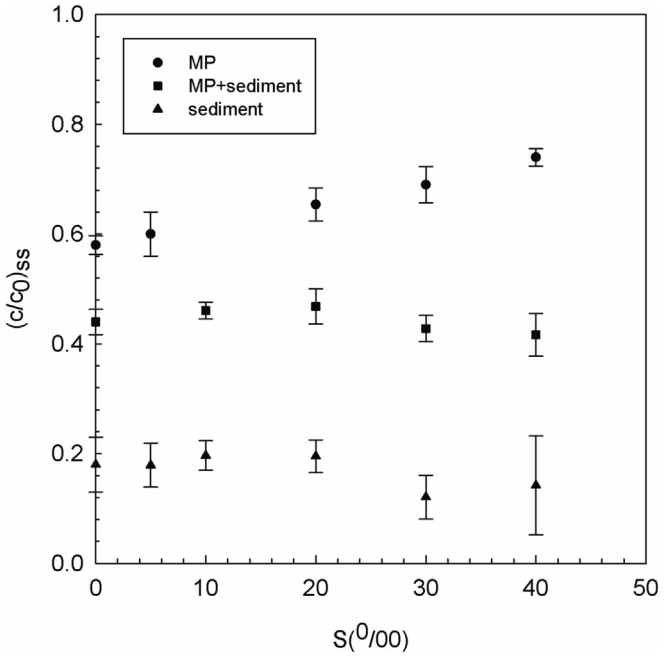

Fig. 6. c/c_0 in the steady state, $(c/c_0)_{ss}$ versus S for G = 0 (s^{-1}) for the different types of suspended particles (MP, sediment, and MP + sediment). Vertical error bars represent the standard deviation of the measurements among the three replicas performed.

lower than k_s for sediment (Fig. 8b). For MP, k_s presents a slight decreasing trend with salinity (Fig. 8a). In contrast, for sediment particles k_s remains constant with salinity (Fig. 8b).

Experimental results were fitted to the model for all the G, for MP and sediment. The total rate of decay was determined and has been plotted in Fig. 9. For both cases MP and sediment, $k_t < 0$; indicating that k_s was greater than k_{res} (Fig. 9). For experiments with MP, k_t was smaller than that for sediment. For both particle types, k_t followed a linear trend with G with a greater slope for the sediment experiments than for MP experiments.

4. Discussion

In this study, we measured the scavenging of MP by sediment particles in calm (non-sheared) and mixing (sheared) fresh and salty water environments to investigate the effects on their removal through both sedimentation and mixing. Suspended sediment particles in the range of 6 μm to 30 μm presented a greater decrease in c/c_0 than MP particles for the same particle range, which can be attributed to the different sedimentation rates caused by the sediment having a greater particle density (2500–2700 kg m^{-3}) compared to the polystyrene MP (1050 kg m^{-3}). For experiments with a mixture of MP and sediment, the rate of decrease in c/c_0 in the range of 6 to 30 μm is smaller than sediment only, but larger than MP only. This result is attributed to the scavenging of MP by sediment particles through the process of differential particle sedimentation. In this case, fast-settling sediment particles would scavenge slow-settling MP particles during their sedimentation, i.e., increasing the transport of MP to the bottom. The transport of MP by fast settling sediment particles was also observed by Li et al. (Li et al., 2019a; Li et al., 2019b). In their work, heteroaggregates of sediment and polystyrene MP and polyethylene MP

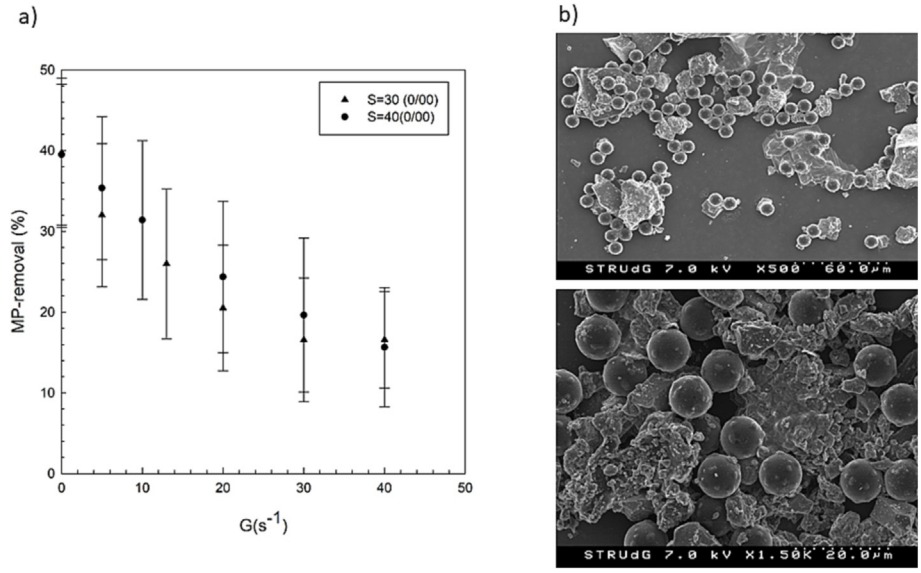

Fig. 7. a) Removal of MP (in %) by sediment particles versus G (in s^{-1}) for S = 30 (‰) and S = 40 (‰). b) Images obtained with the scanning electron microscope (SEM) of settled heteroaggregates of MP and sediment particles at t = 120 min for an experiment carried out with MP and sediment particles at a shear rate of 20 s^{-1}: the upper panel corresponds to an image amplified x500, and the lower panel corresponds to an image amplified ×1500.

formed, thus increasing the transport of MP to the bottom of the water column. However, they conducted all their studies in calm conditions. In the work here conducted, the scavenging of MP by sediment has been found for all the experimental conditions tested, i.e., different salinities and different shear rates. However, c/c_0 increases with the shear rate, indicating that there is particle resuspension in sheared waters compared to non-sheared waters. Then, in environments where the fluid is calm (non-sheared), the removal of particles from the water column is expected to be higher than the removal of particles in turbulent (sheared) environments. For experiments with MP + sediment, the ratio of c/c_0 in the steady state is 0.42 for non-sheared experiments, indicating that fewer MP in suspension than settled at the bottom of the water column are expected to be found, confirming the first hypothesis of the study. Likewise, in the Elbe River Scherer et al. (Scherer et al., 2020) found that the abundance of MP in sediments was 600,000 times that in the water column. However, in sheared environments mixing reduces the settling of MP, with c/c_0 = 0.72 for G = 40 s^{-1}, indicating that MP will remain mainly in the water column, thus confirming the second hypothesis of this work. Chubarenko et al. (Chubarenko et al., 2018) also pointed the important role hydrodynamics has in the transport of MP particles in the water column, showing that mixing in coastal areas can produce the resuspension of deposited MP that can then be transported to other areas by ocean currents. Scavenging has been also observed to enhance the transport and accumulation of heavy metals in the bottom sediments of the Nakivubo Stream (Sekabira et al., 2020), posing a potential pollution hot spot after sediment disturbance. Balistrieri and Murray (Balistrieri and Murray, 1984) found that the scavenging depended on the

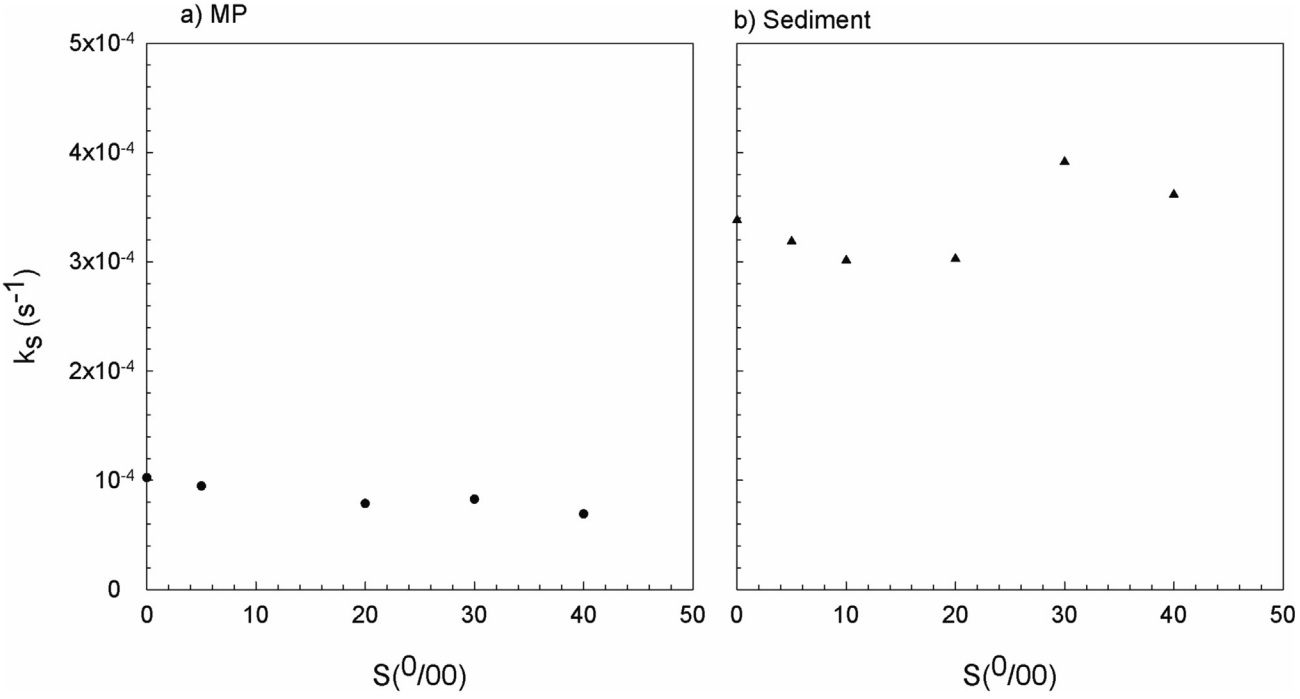

Fig. 8. Sedimentation rate (k_s, in s^{-1}) versus S for G = 0 s^{-1} and for the two different particle types: MP in a) and sediment in b).

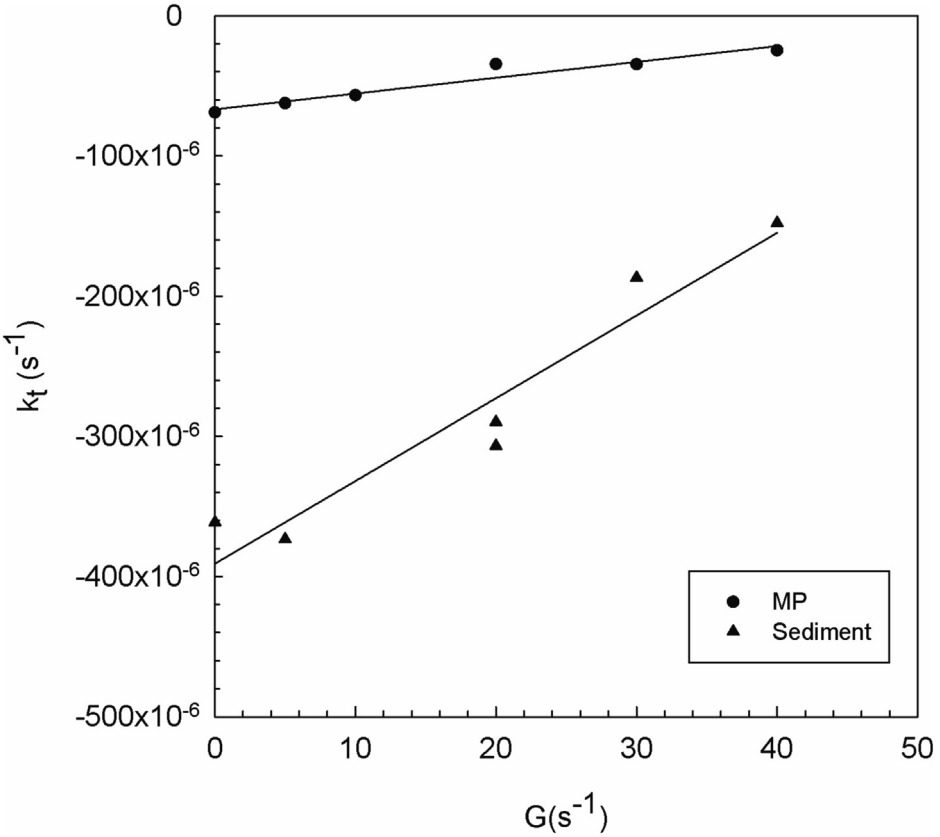

Fig. 9. Total rate of decrease (k_t, in s^{-1}) versus G for S = 40 (‰) and for the two different particle types: MP and sediment.

pH and both sediment and MP concentrations. The sediment characteristics was also found to determine the scavenging of some metals by sediment particles (Baruah et al., 1996). Not only this, but our experiment also describes that the scavenging of MP observed in the water column may mimic the dynamics of snowfall in the atmosphere (Abbasi et al., 2022) with snowfall increasing the vertical transport of atmospheric MP particles (in suspension) that are then transferred to the soil and surface waters.

The scavenging of MP was also investigated for different salinities. For the case of MP only, the concentration of suspended particles increased with the salinity. This was mainly attributed to the fact that these particles became more buoyant in waters with high saline levels as opposed to freshwater environments. It must be noted that the higher water salinities studied produced waters with densities closer to those of MP (1050 kg m^{-3} for MP compared to 1040 kg m^{-3} for the highest level of saline water studied). Jiang et al. (2022) reported the presence of MP in the sediments of Lake Qinghai, with regions with a high salinity presented low abundances of MP in bottom sediments, indicating that they become more buoyant. As such, one can expect to find a higher concentration of MP in freshwater beds than in seabeds. In contrast to this, sediment particles presented a constant concentration for the different salinities tested. Since sediment has a much greater density than water (2500–2700 kg m^{-3} compared to 1040 kg m^{-3} for the highest salinity tested), the effect of salinity on the buoyancy of sediment particles is expected to be negligible. The MP plus sediment mixture showed the rate of decrease in particles remaining constant with the salinity, indicating that the rate of MP transport to the bottom layers depended mainly on the transport of sediment particles. Furthermore, in salt waters, the flux of MP due to the scavenging of sediment is greater than the flux of MP in freshwaters. This is due to the fact that MP + sediment remains constant with salinity whereas in experiments with MP only the concentration of MP increases with salinity. This makes evident the important role of sediment particles in clearing MP from the water column of aquatic ecosystems.

In all the cases tested in the current study, the total rate of decrease k_t was negative. This indicates that k_{res}-$k_{sed} < 0$, i.e., $k_{res} < k_{sed}$. Therefore, for the range of shear rates tested, sedimentation dominates over the resuspension produced by mixing, thus confirming the third hypothesis outlined here. However, k_t was smaller for MP than for sediment particles, indicating that the transport of MP to the bottom sediments was lower than that for sediment particles. For MP, the shear rate for which $k_{res} > k_{sed}$ would be 59.11 s^{-1}. In contrast, for sediment particles, that rate would be 66.27 s^{-1}. That is, the shear rate required to produce resuspension is greater for sediment particles than for MP particles, aligning with the fact that since sediment particles have a higher density and a larger mean diameter than MP particles, they would require a higher shear rate to be able to be resuspended (Roberts et al., 1998). Likewise, in calm conditions, the rate of sedimentation of MP was lower than that of sediment particles, i.e., k_{sed} for sediment was three times that for MP particles.

The percentage of removal of MP in experiments with MP and sediment was always higher than in experiments with MP alone because of sediment scavenging MP, as observed in the photographs of the heteroaggregates between sediment particles and MP particles settled at the bottom of the reactors. Polystyrene MP were actively transported to the bottom by fast-sinking sediment. Scherer et al. (Scherer et al., 2020) found that the concentration of MP in the water column was lower than their concentration in sediments. Therefore, sediments are proven to sink MP in the water column to the bottom, thus aligning with the results of Scherer et al. (Scherer et al., 2020). The percentage of MP particle removal by sediment has been determined to decrease with the shear rate. That is, the transport of MP to the bottom of the water column in mixing environments is expected to be lower than in calm environments. In calm environments, an extra 40 % removal of MP was found due to the presence of sediment, whereas in mixing environments this was 20 %. In this case, mixing reduced the scavenging of MP by sediment, i.e., likewise reducing the transport of MP to the bottom of the water column. No difference was found for the removal of MP by

sediment particles for experiments with different salinities. Therefore, the particle resuspension in sheared environments has been found to be a critical parameter in the removal of MP by sediment particles in the water column, which according to Malli et al. (Malli et al., 2022) can add to other factors such as sedimentation, biofouling, aggregation, salinity gradient and resuspension. In addition, as pointed out by Pinheiro et al. (Pinheiro et al., 2021), differences between plastic particle density and water density are expected to cause buoyancy changes and determine the transport of MP in the water column. Likewise, Vaughan et al. (Vaughan et al., 2017) noted that the distribution of MP particles is dependent on their buoyancy which, in turn, is regulated by biofouling. However, since sediment particles have a density far above the water density, when MP particles are in suspension with sediment particles, the scavenging of MP by sediment particles will determine their vertical transport in the water column.

Therefore, sinking sediment particles play a crucial role in increasing the transport of MP particles in the water column and accumulating them at the bottom sediments. Woodall et al. (Woodall et al., 2014) found that the bottom sediments of ocean basins accumulate four times the observed concentration in the water column. Furthermore, Pohl et al. (Pohl et al., 2020) found that microplastics can also be transported by turbidity currents. However, the current study reveals that MP alone may remain for longer times in the aquatic environment compared to the case where sediment particles are present, in which case the residence time is reduced. Low shear rates produce a higher removal of MP from the water column, i.e., in the absence of turbulence, high amounts of MP are easily transported to the bottom. Likewise, Vianello et al. (Vianello et al., 2013) found that the distribution of MP in bottom sediments was affected by the local hydrodynamics of a lagoon in such a way that MP tended to accumulate in low-dynamic areas, i.e., in the inner areas of the lagoon. The observed interaction between MP particles and suspended sediment particles can also bring clues to understand the patterns of deposited MP in natural environments. For example, river plumes can be a longitudinal transport mechanism for MP particles. However, the presence of suspended sediment might enhance their transport to the bed, explaining the accumulation of small MP particles in river mouths (Bailey et al., 2021). The current manuscript also provides information on the impact of mixing in the transport of MP in the water column in both freshwater and sea, indicating that calm regions along the ecosystems like wetlands or river floodplains are potential hotspots for MP accumulation ((Zhang, 2017).)

Coppock et al. (Coppock et al., 2017) found an effective portable system to extract MP particles from marine sediments based on the flotation of polymers. Therefore, although fine MP particles might be difficult to remove from the water column, MP particle deposited onto sediment might be able to be eliminated effectively. Decontamination of microplastics in aquatic systems needs to be addressed further in the future to find effective technological methods to remove microplastics (Chellesamy et al., 2022). In addition, microplastic litter controls, as well as educational and awareness strategies need to be established to prevent further increases in contamination (Garcés-Ordóñez et al., 2020).

5. Conclusions

The current study demonstrated the interaction between microplastic particles and sediment particles when they are subjected to different salinities and turbulence levels. Sediment particles settle faster and scavenge microplastic particles as they move through the water column, thus producing additional removal of microplastic particles. In calm (non-sheared) environments, greater scavenging of microplastic particles will hold. However, in mixing (sheared) environments, mixing will reduce sediment particle settling and so more microplastic particles will remain in suspension in the water column. Consequently, coastal zones polluted by microplastics and dominated by mixing processes, might represent a source of settled microplastic particles, with more plastics than would be expected. In contrast, calm zones (such as the open ocean, wetlands or the centre of lakes) polluted by microplastics are expected to be a sink of microplastics with a higher microplastic pollution in the bottom sediments.

On the other hand, salinity increased the buoyancy of microplastics in the water column, i.e. reduced the removal of MP. However, in experiments where microplastics were combined with sediments, sediment particle scavenging of microplastics overcame buoyancy, resulting in a constant concentration of suspended microplastics for the different salinities tested. Therefore, microplastic particles that would be expected to remain in suspension with a higher concentration in saline environments were instead transported downwards by fast-sinking sediment particles independent of the water salinity.

Therefore, fast-sinking sediment particles need to be considered in determining the flux of suspended MP particles in both freshwater and seawater ecosystems. In turn, the scavenging of microplastics by sediment is expected to increase the microplastic pollution of sediment beds especially in calm environments independently of the water salinity.

CRediT authorship contribution statement

Conceptualisation (TS and JC), Methodology (TS), Investigation (TS and JC), Writing-original draft (TS), Writing and Editing (TS and JC), Visualization (TS and JC).

Data availability

Data will be available after acceptance of the manuscript

Declaration of competing interest

The authors declare that they have no known competing financial interests or personal relationships that could have appeared to influence the work reported in this paper.

Acknowledgements

This work was supported by the Ministerio de Ciencia e Innovación through the Grant Number PID2021-123860OB-100, and by the European Commission through the project “Plastics monitoRIng detectiOn RemedIaTion recoverY – PRIORITY” COST Action.

Appendix A. Supplementary data

Supplementary data to this article can be found online at https://doi.org/10.1016/j.scitotenv.2023.163720.

References

Abbasi, S., Alirezazadeh, M., Razeghi, N., Rezaei, M., Pourmahmood, H., Dehbandi, R., Mehr, M.R., Ashayeri, S.Y., Oleszczuk, P., Turner, A., 2022. Microplastics captured by snowfall: a study in northern Iran. Sci. Total Environ. 822, 153451.

Andradi, A.L., 2011. Microplastics in the marine environment. Mar. Pollut. Bull. 62, 1596–1605.

Arnott, R.N., Cherif, M., Bryant, L.D., Wain, D.J., 2021. Artificially generated turbulence: a review of phycological nanocosm, microcosm, and mesocosm experiments. Hydrobiologia 848, 961–991.

Bailey, K., Sipps, K., Saba, G.K., Arbuckle-Keil, G., Chant, R.J., Fahrenfeld, N.L., 2021. Quantification and composition of microplastics in the Raritan Hudson estuary: comparison of pathways of entry and implications for fate. Chemosphere 272, 129886.

Balistrieri, L.S., Murray, J.W., 1984. Marine scavenging: trace metal adsorption by interfacial sediment from MANOP site H. Geochim. Cosmochim. Acta 48 (921), 929.

Baruah, N.K., Kotoky, P., Bhattacharyya, K.G., Borah, G.C., 1996. Metal speciation in Jhanji River sediments. Sci. Total Environ. 193, 1–12.

Bellasi, A., Binda, G., Pozzi, A., Galafassi, S., Volta, P., Bettinetti, R., 2020. Microplastic contamination in freshwater environments: a review, focusing on interactions with sediments and benthic organisms. Environments 7, 30.

Browne, M.A., Galloway, T.S., Thompson, R.C., 2010. Spatial patters of plastic debris along estuarine shorelines. Environ. Sci. Technol. 44 (9), 3404–3409.

Chellesamy, G., Kiriyanthan, R.M., Maharajan, T., Radha, A., Yun, K., 2022. Remediation of microplastics using bionanomaterials: a review. Environ. Res. 208, 112724.

Chorom, M., Rengasamy, P., 1995. Dispersion and zeta potential of pure clays as related to net particle charge under varying pH, electrolyte concentration and cation type. Eur. J. Soil Sci. 46, 657.

Chubarenko, I., Esiukova, E., Bagaev, A., Isachenko, I., Demchenko, N., Zobkov, M., Efimova, I., Bagaeva, M., Khatmullina, L., 2018. Behavior of microplastics in coastal zones.

Microplastic Contamination in Aquatic Environmental: An Emerging Matter of Environmental Urgency. Elsevier, pp. 175–223.
Cole, M., Lindeque, P., Fileman, E., Halsband, C., Goodhead, R., Moger, J., Galloway, T.S., 2013. Microplastic ingestion by zooplankton. Environ. Sci. Technol. 47, 6646–6655.
Colomer, J., Contreras, A., Folkard, A., Serra, T., 2019. Consolidated sediment resuspension in model vegetated canopies. Environ. Fluid Mech. 19, 1–24.
Coppock, R.L., Cole, M., Lindeque, P., Queirós, A.M., Galloway, T.S., 2017. A small-scale, portable method for extracting microplastics from marine sediments. Environ. Pollut. 230, 829–837.
Erni-Cassola, G., Zadjelovic, V., Gibson, M.I., Christie-Oleza, J.A., 2019. Distribution of plastic polymer types in the marine environment; a meta-analysis. J. Hazard. Mater. 369, 691–698.
Garcés-Ordóñez, O., Espinosa, L.F., Pereira, R., Costa, M., 2020. The impact of tourism on marine litter pollution on Santa Marta beaches, Colombian Caribbean. Mar. Pollut. Bull. 160, 111558.
Geyer, W.R., Scully, M.E., Ralston, D.K., 2008. Quantifying vertical mixing in estuaries. Environ. Fluid Mech. 8, 495–509.
Gregory, M., 1996. Plastic 'scrubbers' in hand cleansers: a further (an minor) source for marine pollution identified. Mar. Pollut. Bull. 32 (12), 867–871.
Hengstmann, E., Weil, E., Walbott, P.C., Tamminga, M., Fischer, E.K., 2021. Microplastics in lakeshore and lakebed sediments – external influences and temporal and spatial variabilities of concentrations. Environ. Res. 197, 111141.
Hidalgo-Ruz, V., Gutow, L., Thompson, R.C., Thiel, M., 2012. Microplastics in the marine environment: a review of the methods used for identification and quantification. Environ. Sci. Technol. 46 (6), 3060–3075.
Ivar do Sul, J.A., Costa, M.F., 2014. The present and future of microplastic pollution in the marine environment. Environ. Pollut. 185, 352–364.
Jiang, N., Luo, W., Zhao, P., Ga, B., Jia, J., Giesy, J.P., 2022. Distribution of microplastics in benthic sediments of Qinghai Lake on the Tibetan Plateau, China. Sci. Total Environ. 835, 155432.
Leiser, R., Wu, G., Neu, T.R., Wendt-Potthoff, K., 2020. Biofouling, metal sorption and aggregation are related to sinking of microplastics in a stratified reservoir. Water Res. 176, 115748.
Li, D., Peng, G., Zhu, L., 2019. Progress and prospects of marine microplastic research in China. Anthropocene Coasts 2, 330–339.
Li, Y., Wang, X., Fu, W., Xia, X., Liu, C., Min, J., Zhang, W., Crittenden, J.C., 2019. Interactions between nano/micro plastics and suspended sediment in water: implications on aggregation and settling. Water Res. 161, 486–495.
Long, M., Moriceau, B., Gallinari, M., Lambert, C., Huvet, A., Raffray, J., Soudant, P., 2015. Interactions between microplastics and phytoplankton aggregates: impact on their respective fates. Mar. Chem. 175, 39–46.
Magester, S., Barcelona, A., Colomer, J., Serra, T., 2022. Vertical distribution of microplastics in water bodies causes sublethal effects and changes in Daphnia magna swimming behavior. Ecotoxicol. Environ. Saf. 228, 113001.
Malli, A., Corella-Puertas, E., Hajjar, C., Boulay, A.-M., 2022. Transport mechanisms and fate of microplastics in estuarine compartments: a review. Mar. Pollut. Bull. 177, 113553.
Mao, Y., Li, H., Gu, W., Yang, G., Liu, Y., He, Q., 2020. Distribution and characteristics of microplastics in the Yulin River, China: role of environmental and spatial factors. Environ. Pollut. 265, 115033.
Ostle, C., Thompson, R.C., Broughton, D., Gregory, L., Wootton, M., Johns, D.G., 2019. The rise in ocean plastics evidenced from a 60-year time series. Nat. Commun. 10, 1622.
Peters, F., Redondo, J.M., 1997. Turbulence generation and measurement: application to studies on plankton. Sci. Mar. 61, 205–228.
Pinheiro, L.M., Agostini, V.O., Lima, A.R.A., Ward, R.D., Pnho, G.L.L., 2021. The fate of plastic litter within estuarine compartments: an overview of current knowledge for the transboundary issue to guide future assessments. Environ. Pollut. 279, 116908.
Pitarch, J., Falcini, F., Nardin, W., Brando, V.E., Di cicco, A., Marullo, S., 2019. Linking flow-stream variability to grain size distribution of suspended sediment from a satellite-based analysis of the Tiber River plume (Tyrrhenian Sea). Sci. Rep. 9, 19729.
Pohl, F., Eggenhuisen, J.T., Kane, I.A., Clare, M.A., 2020. Transport and burial of microplastics in deep-marine sediments by turbidity currents. Environ. Sci. Technol. 54, 4180–4189.
Pujol, D., Colomer, J., Serra, T., Casamitjana, X., 2012. A model for the effect of submerged aquatic vegetation on turbulence induced by an oscillating grid. Estuar. Coast. Shelf Sci. 114, 23–30.
Redondo-Hasslerham, P.E., Falahudin, D., Peeters, E.T.H.M., Koelmans, A.A., 2018. Microplastic effect thresholds for freshwater benthic macroinvertebrates. Environ. Sci. Technol. 52, 2278–2286.
Roberts, J., Jepsen, R., Gotthard, D., Lick, W., 1998. Effects of particle size and bulk density on erosion of quartz particles. J. Hydraul. Eng. 124, 1261–1267.
Scherer, C., Weber, A., Stock, F., Vurusic, S., Egerci, H., Kochlens, C., Arendt, N., Foeldi, C., Dierkes, G., Wagner, M., Brennholt, N., Reifferscheid, G., 2020. Comparative assessment of microplastics in water and sediment of a large european river. Sci. Total Environ. 738, 139866.
Sekabira, K., Origa, H.O., Basamba, T.A., Mutumba, G., Kakudidi, E., 2020. Assessment of heavy metal pollution in the urban stream sediments and its tributaries. Int. J. Environ. Sci. Technol. 7, 435–446.
Serra, T., Colomer, J., Casamitjana, X., 1997. Aggregation and breakup of particles in a shear flow. J. Colloid Interface Sci. 187, 466–473.
Serra, T., Colomer, J., Logan, B.E., 2008. Efficiency of different shear devices on flocculation. Water Res. 42, 1113–1121.
Serra, T., Müller, M., Colomer, J., 2019. Functional responses of Daphnia magna to zero-mean turbulence. Sci. Rep. 9, 3884.
Shiravani, G., Oberrecht, D., Roscher, L., Kernchen, S., Halbach, M., Gerriets, M., Scholz-Böttcher, B.M., Gerdts, G., Badewien, T.H., Wurpts, A., 2023. Numerical modeling of microplastic interaction with fine sediment under estuarine conditions. Water Res. 231, 119564.
Sun, J., Dai, X., Wang, Q., van Loosdrecht, M.C.M., Ni, B.-J., 2019. Microplastics in wastewater treatment plants. Detection, occurrence and removal. Water Res. 152, 21–37.
Thompson, R.C., Olsen, Y., Mitchell, R.P., Davis, A., Rowland, S.J., John, A.W.G., McGonigle, D., Russell, A., 2004. Lost at sea: Where is all the plastic? Science 304 (5672), 838.
Thompson, R.C., Swan, S.H., Moore, C.J., vom Saal, F.S., 2009. Our plastic age. Philos. Trans. R. Soc. B 364, 1973–1976.
Tosetto, L., Brown, C., Williamson, J.E., 2016. Microplastics on beaches: ingestion and behavioural consequences for beachhoppers. Mar. Biol. 163, 199.
Van Cauwenberghe, L., Vanresusel, A., Mees, J., Janssen, C.R., 2013. Microplastic pollution in deep-sea sediments. Environ. Pollut. 182, 495–499.
Vaughan, R., Turner, S.D., Rose, N.L., 2017. Microplastics in the sediments of a UK urban lake. Environ. Pollut. 229, 10–18.
Vianello, A., Boldrin, A., Guerriero, P., Moschino, V., Rella, R., Sturaro, A., Da Ros, L., 2013. Microplastic particles in sediments of lagoon Venice, Italy: first observations on occurrence, spatial patterns and identification. Estuar. Coast. Shelf Sci. 130, 54–61.
Woodall, L.C., Sanchez-Vidal, A., Canals, M., Paterson, G.L.J., Coppock, R., Sleight, V., Calafat, A., Rogers, A.D., Narayanaswamy, B.E., Thompson, R.C., 2014. The deep sea is a major sink for microplastic debris. R. Soc. Open Sci. 1, 140317.
Xia, F., Yao, Q., Zhang, J., Wang, D., 2021. Effects of seasonal variation and resuspension on microplastics in river sediments. Environ. Pollut. 286, 117403.
Yuan, Z., Nag, R., Cummins, E., 2022. Ranking of potential hazards from microplastics polymers in the marine environment. J. Hazard. Mater. 429, 128399.
Zhang, H., 2017. Transport of microplastics in coastal seas. Estuar. Coast. Shelf Sci. 199, 74–86.